2). Anal. Calcd for $C_{15}H_{11}O_2Br$: C, 59.41; H, 3.63; Br, 26.40. Found: C, 59.29; H, 3.47; Br, 26.75.

Preparation of Carbocation 2 under Stable Ion Conditions. Methyl 9-bromofluorene-9-carboxylate (**4a**) (100.0 mg) was dissolved in 1.0 mL of SO_2 in a 10-mm NMR tube. This was mixed with SbF_5/SO_2 at -78 °C. A reddish-brown color was observed, ^{13}C NMR: δ 67.4 (OCH_3), 124.5-145.6 (aromatic), 174.2 (C=O), 192.4 (C^+).

Quenching of Carbocation 2 with CH_3OH. A solution of 70.0 mg of methyl 9-bromofluorene-9-carboxylate (**4a**) dissolved in 10.0 mL of dry dichloromethane was prepared. To this solution was added 100.0 mg (1.2 equiv) of silver hexafluoroantimonate in 1.0 mL of dichloromethane. A red color was observed, and silver bromide was formed as a precipitate. The solution was quenched with methanol immediately. The solvent was removed by reduced pressure, and 48.0 mg (83%) of methyl 9-methoxyfluorene-9-carboxylate (**4c**) was obtained (R_f 0.38): ^1H NMR ($CDCl_3$, 300 MHz) δ 2.94 (s, 3 H, OCH_3), 3.68 (s, 3 H, OCH_3); 7.38 (m, 2 H, aromatic), 7.51 (m, 4 H, aromatic), 7.75 (d, 2 H, J = 7.83 Hz, aromatic); ^{13}C NMR δ 51.2 (OCH_3), 53.7 (OCH_3), 87.8 (quaternary), 120.6, 124.1, 128.0, 130.2 (CH, aromatic), 140.5, 141.7 (aromatic, quaternary), 173.7 (C=O): HRMS (M^+) calcd for $C_{16}H_{14}O_3$ 254.0939, found 254.0927. Anal. Calcd for $C_{16}H_{14}O_3$: C, 75.59; H, 5.51. Found: C, 75.27; H, 5.35.

Quenching of Carbocation 2 with Benzene. To a solution of 30.0 mg of methyl 9-bromofluorene-9-carboxylate (**4a**) in 3.0 mL of SO_2 at -75 °C was added a few drops of SbF_5 in SO_2. The solution was quenched with dry benzene at -75 °C. The mixture was allowed to warm up to -20 °C. The reaction mixture was poured onto ice, saturated sodium bicarbonate was added, and the ice was allowed to melt. The aqueous layer was extracted with benzene (20 mL), and the organic layer was dried by addition of $MgSO_4$. The solvent was removed by reduced pressure. The reaction mixture was applied on preparatory thin-layer chromatography plates (silica gel) and developed in dichloromethane to give compound **6a** (R_f 0.86; 59%): mp 157-159 °C; ^1H NMR ($CDCl_3$, 300 MHz) δ 3.75 (s, 3 H, OCH_3), aromatic protons 7.13 (m, 2 H), 7.23 (m, 3 H), 7.30 (t, 2 H), 7.40 (t, 2 H), 7.59 (d, 2 H, J = 7.6 Hz), 7.75 (d, 2 H, J = 7.49 Hz); ^{13}C NMR δ 52.9 (OCH_3), 67.3 (quaternary), 120.0, 126.7, 127.1, 127.9, 128.4, 128.8 (CH, aromatic), 140.8, 141.9, 146.1 (aromatic, quaternary), 172.5 (C=O); MS, m/e 241, 300 (M^+ base peak); HRMS (M^+) calcd for $C_{21}H_{16}O_2$ 300.1150, found 300.1137. Anal. Calcd for $C_{21}H_{16}O_2$: C, 84.00; H, 5.33. Found: C, 83.71; H, 5.48.

Quenching of Carbocation 2 with Toluene. To a solution of 30.0 mg of methyl 9-bromofluorene-9-carboxylate (**4a**) in 3.0 mL of SO_2 at -78 °C was added a few drops of SbF_5 in SO_2. The solution was quenched with dry toluene at -78 °C. The mixture was allowed to warm up to -20 °C. The reaction mixture was poured onto ice, saturated sodium bicarbonate was added, and the ice was allowed to melt. The aqueous layer was extracted with toluene (20 mL), and the organic layer was dried over $MgSO_4$. The solvent was removed by reduced pressure. The reaction mixture was applied on preparatory thin-layer chromatography plates (silica gel) and developed in dichloromethane to give compound **6b** (R_f 0.90; 56%): mp 128-130 °C; ^1H NMR ($CDCl_3$, 300 MHz) δ 3.75 (s, 3 H, OCH_3), aromatic protons 7.13 (m, 2 H), 7.23 (m, 3 H), 7.30 (t, 2 H), 7.40 (t, 2 H), 7.59 (d, 2 H, J = 7.6 Hz), 7.75 (d, 2 H, J = 7.49 Hz) ^{13}C NMR δ 20.9 (CH_3), 52.8 (OCH_3), 67.3 (quaternary), 120.0, 126.5, 126.9, 127.7, 128.2, 129.3 (CH, aromatic), 137.0, 138.8, 140.6, 146.2 (aromatic, quaternary), 172.6 (C=O); HRMS calcd for $C_{22}H_{18}O_2$ 314.1307, found 314.1295. Anal. Calcd for $C_{22}H_{18}O_2$: C, 84.08; H, 5.73. Found: C, 83.69; H, 5.47.

Continuous Irradiation of Bromides 3a and 4b. A solution containing either **3a** or **4a** (100 mg) in 10 mL of methanol was irradiated for 30 min. The reaction mixture was evaporated to dryness, and the residue was applied on one thin layer chromatography plate and eluted with methylene chloride. A solution of bromide **3a** or **4a** in 50% aqueous acetonitrile was irradiated under identical conditions, and the products were separated as above.

Photoproducts **3b**, **3c**, **3d**, **10b**, **4b**, **4c**, and **4d**,[30] were compared with authentic samples obtained commercially or prepared by literature methods.

Laser Flash Photolysis. Either a Lumonics HY750 Nd:YAG laser (355 or 266 nm; 10-ns pulses; ≤50 mJ/pulse) or a Lumonics EX-510 excimer laser (XeCl, 308 nm, 6-ns pulse, ≤40 mJ/pulse) was used for sample excitation. Solutions were contained in 7 × 7 mm^2 quartz cells (quenching experiments) or in 7 × 7 mm^2 flow-through cells connected with Teflon-brand tubing to a sample reservoir (spectra). For some experiments the samples were deaerated by purging with either nitrogen or oxygen before and during the experiment. The rate constants for reaction of cation **2** with nucleophiles were determined using aerated samples. The rest of the laser system is as described previously,[31] except for the use of a PC-386 computer for data acquisition.

Acknowledgment. E.L.-R. would like to thank the Natural Science and Engineering Research Council of Canada (NSERC) for their generous support.

(30) Bergmann, E.; Schuchdart, W. *Justus Liebigs Ann. Chem.* **1931**, *487*, 225.

(31) Kazanis, S.; Azarani, A.; Johnston, L. J. *J. Phys. Chem.* **1991**, *95*, 4430.

Novel Cage Molecules from the Reaction of 8,8-Dicyanoheptafulvene with Cyclopentadienide Anion: Structure and Mechanism[1,2]

Takahisa Machiguchi,*[,3a] Shinichi Yamabe,*[,3b] Tsutomu Minato,[3c] Toshio Hasegawa,[3a] and Toyonobu Asao*[,3d]

Contribution from the Department of Chemistry, College of Liberal Arts and Science, Saitama University, Shimo-Ohkubo, Urawa, Saitama 338, Japan, Educational Technology Center, Nara University of Education, Takabatake-cho, Nara, Nara 630, Japan, Institute for Natural Science, Nara University, Misasagi-cho, Nara, Nara 631, Japan, and Department of Chemistry, College of General Education, Tohoku University, Kawauchi, Aoba-ku, Sendai, Miyagi 980, Japan.
Received May 27, 1992

Abstract: The reaction of 8,8-dicyanoheptafulvene and sodium cyclopentadienide affords under mild conditions two unusual tetracyclic cage molecules with (dicyanomethylene)tetracyclo[7.2.1.0.0]dodecadiene structures. The structures were elucidated using various modern NMR spectroscopic techniques and deuterium-labeling experiments. The easy formation of the considerably strained molecules is ascribed to a nucleophilic addition, followed by protonation and an intramolecular Diels–Alder reaction with normal electron demand. MNDO-MO calculations suggest a possible reaction mechanism.

In clear contrast to the thermally unstable heptafulvene,[4] 8,8-dicyanoheptafulvene[5] (**1**) is characterized by a relatively large dipole moment (μ = 7.49 D)[6] as well as by considerable π-delocalization, on the basis of an X-ray diffraction study.[7] The

0002-7863/93/1515-1669$04.00/0

Scheme I

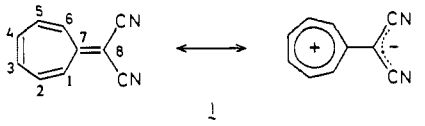

1

Scheme II

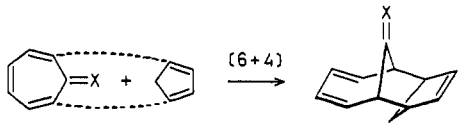

1 X = C(CN)$_2$ 3 4 X = C(CN)$_2$
2 X = O 5 X = O

Scheme III

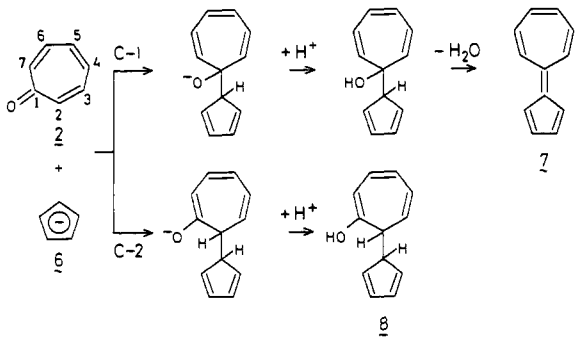

structurally similar molecule tropone[8] (**2**) readily undergoes a variety of cycloaddition reactions,[9,10] and indeed both **1** and **2** react with cyclopentadiene (**3**) to give the same [6 + 4]-type of cycloadduct **4**[11] and **5**,[12] respectively. However, tropone reacts with cyclopentadienide anion (**6**) to give sesquifulvalene (**7**) and 2-cyclopentadienylcyclohepta-3,5,7-trienol (**8**) by nucleophilic attack on the C-1 and C-2 positions of **2**, respectively,[13] which is different from the result obtained with **1** that we report here.

Scheme IV

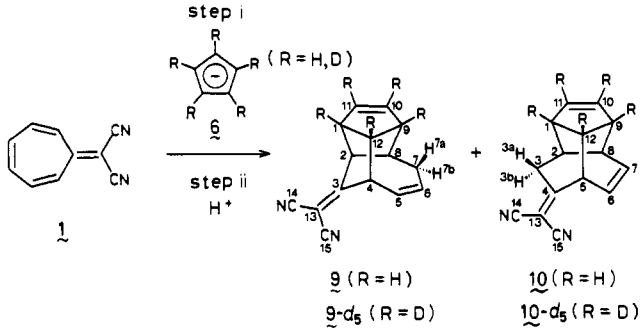

Reaction of **1** with **6** under mild conditions affords two unusual cycloadducts **9** and **10**, both of which have relatively high strain.

The deuterium-substituted cyclopentadienide anion (**6**-d_5) was used to determine the structures of **9** and **10** unequivocally by NMR studies. We also have performed MO calculations based on FMO theory to clarify the differences in reactivity between **1** and **2** (Schemes II–IV).

Results

Reaction of 8,8-dicyanoheptafulvene (**1**) with sodium cyclopentadienide (**6**) in tetrahydrofuran (THF) at −30 °C, followed by neutralization with HCl at −10 °C, gave a mixture of two products **9** (58–69% yield) and **10** (15–28%) separated by preparative thin layer chromatography. Elemental analyses and mass spectrometry (M^+ m/z 220) showed that the products were 1:1 adducts.

The IR spectra of both products **9** and **10** showed very strong absorption at around 2230 cm^{-1}, indicating the presence of conjugated cyano groups, and the UV–visible spectra (see Experimental Section) were consistent with the presence of an $\alpha,\beta,\delta,\epsilon$-homoconjugated diene moiety, on the basis of two reference compounds: (dicyanomethylene)cyclohexane[14] (α,β-conjugation system) and (dicyanomethylene)cyclohexene[15] ($\alpha,\beta,\gamma,\delta$-conjugation system).

We finally established the structures of **9** and **10** from NMR spectroscopic data, together with an examination of the deuteriated products **9**-d_5 and **10**-d_5 (R = D, Scheme IV). The 400-MHz ^{1}H and 100.6-MHz ^{13}C NMR spectra of the products **9** and **10** are too complex for accurate analysis of the couplings (J_{H-H} and J_{C-H}). Both products form a complex network of NMR couplings including long-range ones and several small couplings of unequal magnitudes, which cause broadening of the signals. In order to simplify such spectra, the partially deuteriated adducts **9**-d_5 (isotopic purity: d_5, 94.3%, d_4, 2.9%, from mass spectrometry) and **10**-d_5 (isotopic purity: d_5, 96.1%, d_4, 2.6%) have also been

(1) Dedicated to Professor Tetsuo Nozoe on the occasion of his 90th birthday and a life-long career in novel aromatic chemistry. For his biography, see: Nozoe, T. Seventy Years in Organic Chemistry. In Profiles, Pathways, and Dreams: Autobiographies of Eminent Chemists; Seeman, J. I., Ed.; American Chemical Society: Washington, DC, 1991.

(2) Abbreviations used: 2D, two-dimensional; COSY, shift-correlation spectroscopy; COLOC, shift-correlation spectroscopy by long-range couplings; CPD, composite decoupling; SEL, selective proton decoupling; LSPD, long-range selective proton decoupling; MO, molecular orbital; FMO, frontier MO; MNDO, modified neglect of differential overlap.

(3) (a) Saitama University. (b) Nara University of Education. (c) Nara University. (d) Tohoku University.

(4) Doering, W. E.; Wiley, D. W. *Tetrahedron* **1960**, *11*, 183–198. Matterson, D. S.; Drysdale, J. J.; Sharkey, W. H. *J. Am. Chem. Soc.* **1960**, *82*, 2853–2857. Neuenschwander, M.; Schenk, W. K. *Chimia* **1972**, *26*, 194–197. Hollenstein, R.; von Philipsborn, W.; Vogeli, R.; Neuenschwander, M. *Helv. Chim. Acta* **1973**, *56*, 847–860. Hollenstein, R.; Mooser, A.; Neuenschwander, M.; von Philipsborn, W. *Angew. Chem.* **1974**, *86*, 595–596. Schenk, W. K.; Kyburz, R.; Neuenschwander, M. *Helv. Chim. Acta* **1975**, *58*, 1099–1119. Bauder, A.; Keller, C.; Neuenschwander, M. *J. Mol. Spectrosc.* **1976**, *63*, 281–287. Neuenschwander, M. *Pure Appl. Chem.* **1986**, *58*, 55–66.

(5) (a) Nozoe, T.; Mukai, T.; Osaka, K. *Bull. Chem. Soc. Jpn.* **1961**, *34*, 1384–1390. (b) Kitahara, Y.; Doi, K. Japan Patent 13 071, 1962; *Chem. Abstr.* **1963**, *59*, 9914f. Oda, M.; Funamizu, M.; Kitahara, Y. *Bull. Chem. Soc. Jpn.* **1969**, *42*, 2386–2387. (c) Machiguchi, T.; Okuma, K.; Hoshino, M.; Kitahara, Y. *Tetrahedron Lett.* **1973**, 2011–2012.

(6) Yamakawa, M.; Watanabe, H.; Mukai, T.; Nozoe, T.; Kubo, M. *J. Am. Chem. Soc.* **1960**, *82*, 5665–5667.

(7) Shimanouchi, H.; Ashida, T.; Sasada, Y.; Kakudo, M.; Murata, I.; Kitahara, Y. *Bull. Chem. Soc. Jpn.* **1966**, *39*, 2322–2331.

(8) Bertelli, D. J.; Andrews, T. G.; Crews, P. O. *J. Am. Chem. Soc.* **1969**, *91*, 5286–5296.

(9) For a comprehensive review, see: Asao, T.; Oda, M. In *Carbocyclische π-Elektronen-Systeme: Houben-Weyl, Methoden der organischen Chemie*; Müller, E., Bayer, O., Eds.; Georg Thieme: Stuttgart, Germany, 1986; Vol. 5/2c, pp 49–85, 710–780.

(10) See recent reports on cycloadditions of troponoid compounds and references therein, e.g.: Garst, M. E.; Roberts, V. A.; Houk, K. N.; Rondan, N. G. *J. Am. Chem. Soc.* **1984**, *106*, 3882–3884. Liu, C.-Y.; Smith, D. A.; Houk, K. N. *Tetrahedron Lett.* **1986**, *27*, 4881–4884. Funk, R. L.; Bolton, G. L. *J. Am. Chem. Soc.* **1986**, *108*, 4655–4657. Trost, B. M.; Seoane, P. R. *J. Am. Chem. Soc.* **1987**, *109*, 615–617. Reingold, I. D.; Kwong, K. S.; Menard, M. M. *J. Org. Chem.* **1989**, *54*, 708–710. Machiguchi, T.; Hasegawa, T.; Itoh, S.; Mizuno, H. *J. Am. Chem. Soc.* **1989**, *111*, 1920–1921.

(11) Kitahara, Y.; Oda, M. Aromaticity, Pseudo-Aromaticity, Anti-Aromaticity. *Proceedings of the Jerusalem Symposia on Quantum Chemistry and Biochemistry, III*; The Israel Academy of Sciences and Humanities: Jerusalem, 1971; p 284.

(12) Cookson, R. C.; Drake, B. V.; Hudec, J.; Morrison, A. *J. Chem. Soc., Chem. Commun.* **1966**, 15–16. Itô, S.; Fujise, Y.; Okuda, T.; Inoue, Y. *Bull. Chem. Soc. Jpn.* **1966**, *39*, 1351. Tanida, H.; Pfaendler, H. R. *Helv. Chim. Acta* **1972**, *55*, 3062–3064.

(13) Prinzbach, H.; Rosswog, W. *Angew. Chem.* **1961**, *73*, 543. Neuenschwander, M.; Schenk, W. K. *Chimia* **1972**, *26*, 194–197. Prinzbach, H.; Seip, D.; Knothe, L.; Faisst, W. *Liebigs Ann. Chem.* **1966**, *698*, 34–56. Prinzbach, H.; Schneider, H.-W. *Angew. Chem.* **1973**, *85*, 1112–1113. Kitahara, Y.; Murata, I.; Katagiri, S. *Angew. Chem.* **1965**, *77*, 345–346. Sasada, Y.; Shimanouchi, H.; Murata, I.; Tajiri, A.; Kitahara, Y. *Tetrahedron Lett.* **1969**, 1185–1188.

(14) λ_{max} 235 nm (log ϵ 4.17). Weir, M. R. S.; Hyne, J. B. *Can. J. Chem.* **1963**, *41*, 2905–2908.

(15) λ_{max} 289 nm (log ϵ 4.23). Ref 11. Oda, M.; Kamijyo, M.; Funamizu, M.; Kitahara, Y. *Abstracts of Papers*, 2nd Symposium on Nonbenzenoid Aromatic Chemistry, Kyoto; Chemical Society of Japan: Tokyo, 1968; Abstract 28.

analyzed. Tables I and II display selected data from the ^{13}C and ^{1}H NMR spectra for **9**, **10**, **9**-d_5, and **10**-d_5.

The products **9** and **10** are assigned to be tetracyclic compounds by comparison of the chemical shifts and multiplicities of the undeuteriated adducts (**9** and **10**) and the deuteriated ones (**9**-d_5 and **10**-d_5). The ^{13}C NMR spectra show the presence of two olefinic carbons and three methine carbons derived from cyclopentadienide, as well as two olefinic carbons, one methylene, three methines, and a *gem*-dicyanoethylene moiety derived from 8,8-dicyanoheptafulvene (**1**).

To assign the individual signals (^{13}C and ^{1}H) and spin–spin couplings (J_{CH} and $J_{H,H}$) of the products **9**, **10**, **9**-d_5, and **10**-d_5 the following spectroscopic methods[16] were used: for all protons, Lorentz-transformed ^{1}H NMR and those resolution-enhanced with Gaussian and sine-bell wind functions, separately, 2D NMR ^{1}H–^{1}H COSY,[2,17] and ^{1}H–^{1}H homonuclear double resonance experiments; for long-range ^{1}H–^{1}H couplings, 2D NMR ^{1}H–^{1}H COLOC[18] and ^{1}H–^{1}H decoupling experiments; for all carbons, ^{13}C NMR with CPD and those with proton off-resonance decoupling, ^{13}C–^{1}H SEL, normal gated decoupling, and 2D NMR ^{13}C–^{1}H COSY;[19] for long-range ^{13}C–^{1}H couplings, 2D ^{13}C–^{1}H COLOC,[20] gated decoupling with resolution enhancement using a Gaussian wind function, and ^{13}C–^{1}H LSPD[21] experiments. The ^{13}C–^{1}H long-range couplings were analyzed by the 2D ^{13}C–^{1}H COLOC technique, acquired in three different conditions of polarization delays, and by resolution-enhanced LSPD ones with a Gaussian wind function. Most of the NMR spectroscopic data are provided in the supplementary material.

In the ^{1}H NMR spectrum of **9**-d_5, the olefinic resonances at δ 6.40 and 5.91 and the aliphatic ones at δ 3.08, 2.59, and 2.49, which were observed in **9**, are all absent. We therefore assign the former two resonances to H(10) and H(11), respectively, and the latter three to H(1), H(12), and H(9), respectively. (See Scheme IV for the atom numbering). In the aliphatic proton region, the two signals shifted downfield to δ 3.34 (d) and 3.04 (dd) are assigned to H(4) and H(2), respectively, which are the terminal protons of the coupling system for **9**-d_5. Since these two protons are adjacent to a strongly electron withdrawing *gem*-dicyanoethylene group [C(3)=C(13)$(CN)_2$], they are deshielded and are disposed in a W-type arrangement with a small coupling of $J_{2,4}$ = 1.5 Hz. This arrangement is confirmed by J_{CH} analysis showing $^{3}J_{C(2)H(4)}$, $^{3}J_{C(4)H(2)}$, $^{2}J_{C(3)H(2)}$, $^{2}J_{C(3)H(4)}$, $^{3}J_{C(13)H(2)}$, and $^{3}J_{C(13)H(4)}$ (Table I).

In the ^{1}H NMR spectrum of **9**, the two broad singlets at δ 3.08 and 2.49 are assigned to H(1) and H(9), respectively, and the triplet at δ 2.02 to H(8). The vicinal coupling constants—$J_{1,2}$, $J_{4,12}$, $J_{7a,8}$, $J_{7b,8}$, and $J_{8,9}$—are fully consistent with dihedral angles of 80°, 35°, 21°, 109°, and 85°, respectively, measured by a Dreiding model. For the small coupling of $J_{1,2}$ in **9**, the C(1)–C(2) linkage is confirmed by the $^{3}J_{C(2)H(11)}$, $^{3}J_{C(2)H(12)}$, $^{3}J_{C(11)H(2)}$, and $^{3}J_{C(12)H(2)}$ couplings in Table I. Similarly, for the coupling of $J_{8,9}$, the C(8)–C(9) bond is confirmed by the $^{3}J_{C(7)H(9)}$, $^{3}J_{C(8)H(10)}$, $^{3}J_{C(9)H(7a)}$, $^{3}J_{C(9)H(7b)}$, and $^{3}J_{C(10)H(8)}$ couplings. The 2D NMR ^{1}H–^{1}H COSY, ^{1}H–^{1}H COLOC, and ^{1}H–^{1}H decoupling results (Table II) indicate long-range interactions between H(1) and H(9), H(2) and H(12), and H(8) and H(12) and reflect their W-type arrangement. These arrangements are further verified by $^{3}J_{CH}$ couplings [$J_{C(1)H(9)}$, $J_{C(2)H(12)}$, $J_{C(12)H(2)}$, $J_{C(8)H(12)}$, and $J_{C(12)H(8)}$] (Table I).

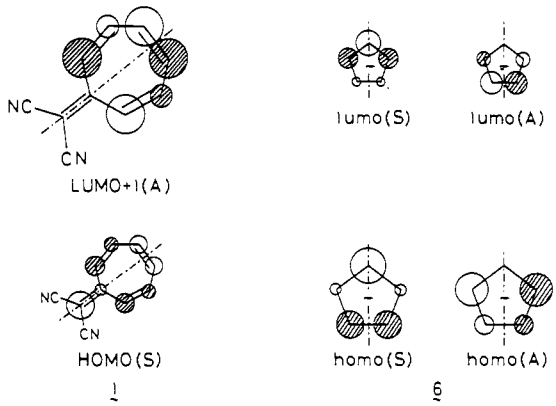

Figure 1. FMOs of **1** and **6** for the step i in Scheme IV. The orbital energies of homo's and lumo's of **6** are −2.14 and 7.94 eV. Those of the HOMO and LUMO+1 (the next LUMO) belonging to **1** are −8.85 and −1.19 eV, respectively. Abbreviations S and A in parentheses attached to FMOs denote symmetric and antisymmetric MOs, respectively, with respect to the mirror plane. The LUMO of **1** has an energy of −1.47 eV and is symmetric (S). This is the FMO for the C-1 attack in Scheme III, but is not concerned with the present cage-molecule formation (see ref 23).

Scheme V

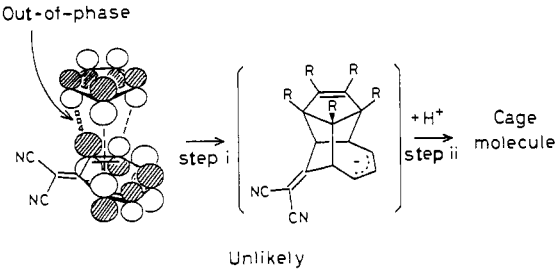

The structure of the byproduct **10** was analyzed in a similar fashion. The olefinic protons at δ 6.15 and 6.11 are ascribed to H(10) and H(11) protons, respectively, which are coupled to allylic H(9) and H(1) protons, respectively. The aliphatic resonance shifted downfield to δ 3.83 is assigned to the bridgehead proton H(5), which, as in the case of **9**, is adjacent to a neighboring ethylene group [C(6)=C(7) bond] and the electron-withdrawing *gem*-dicyanoethylene [C(4)=C(13)$(CN)_2$] group. The proton H(5) is coupled to the vicinal methine proton H(12) by a coupling constant of 8.2 Hz, compatible with a dihedral angle of 2°, and to the vicinal olefinic proton H(6). The UV–visible maxima are also consistent with this configuration. The other vicinal coupling constants—$J_{1,2}$, $J_{1,12}$, $J_{2,3a}$, $J_{2,3b}$, $J_{8,9}$, and $J_{9,12}$—are fully consistent with dihedral angles of 80°, 45°, 40°, 55°, 85°, and 68°, respectively, measured by a Dreiding model. Small long-range interactions between H(1) and H(9), H(2) and H(12), H(3a) and H(5), and H(8) and H(12) are observed in both the 2D NMR ^{1}H–^{1}H COLOC and homonuclear decoupling experiments. This result indicates their respective W-type arrangement. The relationship is further confirmed by $^{3}J_{CH}$ couplings [$J_{C(1)H(9)}$, $J_{C(2)H(12)}$, $J_{C(12)H(2)}$, $J_{C(3)H(5)}$, $J_{C(5)H(3a)}$, $J_{C(8)H(12)}$, and $J_{C(12)H(8)}$] (Table I).

The mass spectra (see Experimental Section) of both the products **9** and **10** display a very similar pattern. The most important fragment peaks appear at m/z 155 ($C_{10}H_7N_2^+$) and 65 ($C_5H_5^+$), which are attributable to a retro-Diels–Alder ring opening followed by cleavage of the C(4)–C(12) bond in **9** and the C(5)–C(12) linkage in **10**.[22]

(16) For an interpretation of modern NMR techniques, see: Derome, A. E. In *Modern NMR Techniques for Chemistry Research*; Baldwin, J. E., Ed.; Organic Chemistry Series 6; Pergamon: Oxford, England, 1987.

(17) Aue, W. P.; Bartholdi, E.; Ernst, R. R. *J. Chem. Phys.* **1976**, *64*, 2229–2246. Nagayama, K.; Kumar, A.; Wuethrich, K.; Ernst, R. R. *J. Magn. Reson.* **1980**, *40*, 321–334.

(18) Bax, A.; Freeman, R. *J. Magn. Reson.* **1981**, *44*, 542–561.

(19) Maudsley, A. A.; Ernst, R. R. *Chem. Phys. Lett.* **1977**, *50*, 368–372. Freeman, R.; Morris, G. A. *J. Chem. Soc., Chem. Commun.* **1978**, 684–686.

(20) Bermel, W.; Griesinger, C. *J. Magn. Reson.* **1984**, *57*, 331–336. Kessler, H.; Griesinger, C.; Zarbock, J.; Loosli, H. R. *J. Am. Chem. Soc.* **1985**, *107*, 1083–1084.

(21) Takeuchi, S.; Uzawa, J.; Seto, H.; Yonehara, H. *Tetrahedron Lett.* **1977**, *18*, 2943–2946. Seto, H.; Sasaki, T.; Yonehara, H.; Uzawa, J. *Tetrahedron Lett.* **1978**, *19*, 923–926.

(22) The fragment peaks at m/z 155 form $C_{10}H_6N_2^+$ species (m/z 154), giving the base peak in **10** and a very intense one in **9** through the loss of hydrogen. These are typical fragmentation patterns of the 8,8-dicyanoheptafulvene skeleton, which produces a (cyanoethynyl)benzene cation radical (m/z 127) through the elimination of HCN followed by further elimination to a benzenium cation (m/z 77). The fragment peaks at m/z 65 in **9** and **10** due to cyclopentadienylium cation form the cyclopropenylium cation radical (m/z 39) by the loss of acetylene. The mass spectra of the deuteriated products, **9**-d_5 and **10**-d_5 were also consistent.

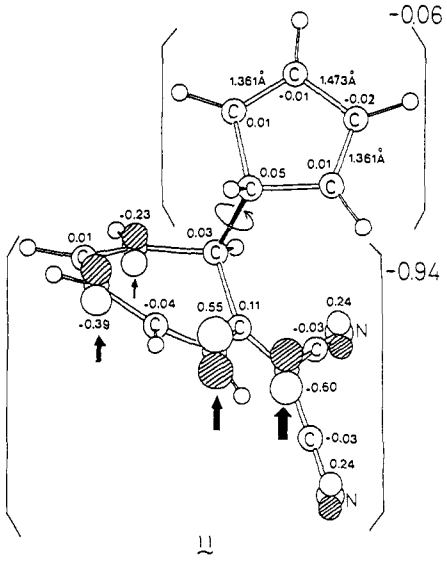

Figure 2. MNDO optimized geometry of the one-centered adduct **11**, generated from reaction of **1** and **6**, together with the shape and coefficient of its HOMO. Small empty circles stand for hydrogen atoms. The values outside the two brackets show the net changes of the cyclopentadienyl moiety and the **1** part. These charges (−0.06 and −0.94) indicate that negative (anionic) density is shifted from the five-membered ring to the **1** skeleton through the one-site addition **1** + **6** → **11**. Note that the five-membered ring is of the cyclopentadiene structure. Upward arrows denote protonation sites, size shown relative to probability.

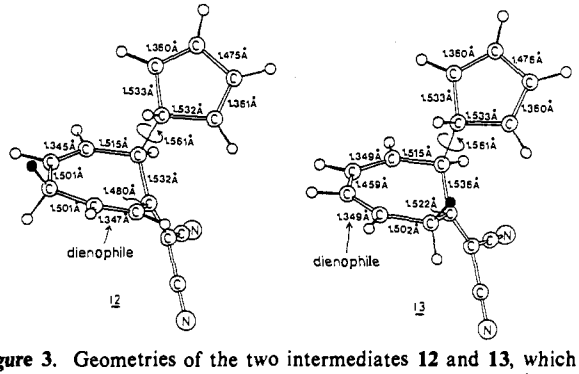

Figure 3. Geometries of the two intermediates **12** and **13**, which are obtained by the protonation of **11** according to the FMO predictions in Figure 2. The attached proton is denoted by a black circle.

On the basis of these spectroscopic results, we have unequivocally established the structures of the main product **9** to be 3-(dicyanomethylene)tetracyclo[7.2.1.$0^{2,8}$.$0^{4,12}$]dodeca-5,10-diene and the minor adduct **10** to be 4-(dicyanomethylene)tetracyclo-[7.2.1.$0^{2,8}$.$0^{5,12}$]dodeca-6,10-diene.

Discussion

The first mechanistic question is whether or not the cage molecules **9** and **10** have been obtained in one step via a concerted three-bond formation. To examine this possibility, FMOs of **1** and **6** are drawn in Figure 1. (HOMO and homo stand for the highest occupied MOs of **1** and **6**, respectively. LUMO and lumo denote the lowest unoccupied MOs of **1** and **6**, respectively). We tested various (LUMO+1)–homo overlaps to find effective **6** → **1** charge transfer (CT). However, no reasonable stacking approach can be found in which there is sufficient overlap or bond interchanges on the basis of the FMO nodal properties. The absence of an in-phase FMO overlap or of reasonable bond interchanges indicates that the concerted formation of **9** and **10** is unlikely, as is shown in Scheme V.

MNDO geometry optimization on the **1**–**6** interacting system gives the anionic intermediate **11** in Figure 2.[23] This initial

Scheme VI

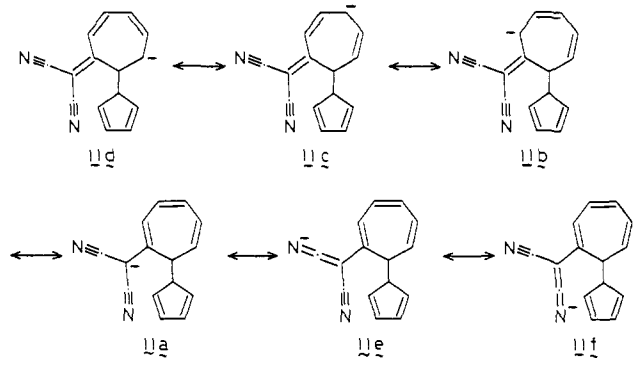

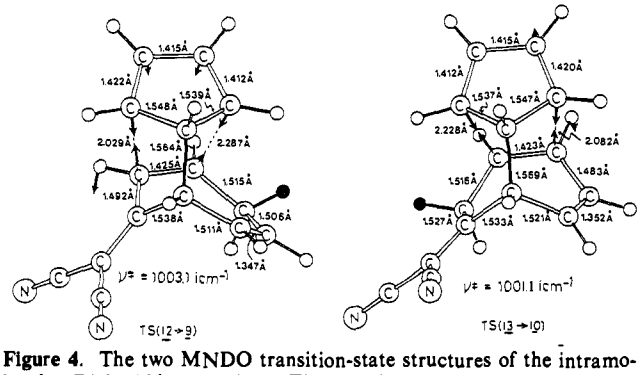

Figure 4. The two MNDO transition-state structures of the intramolecular Diels–Alder reaction. The reaction coordinate vector corresponding to the imaginary frequency ν^* indicates that a synchronous C–C bond formation is likely.

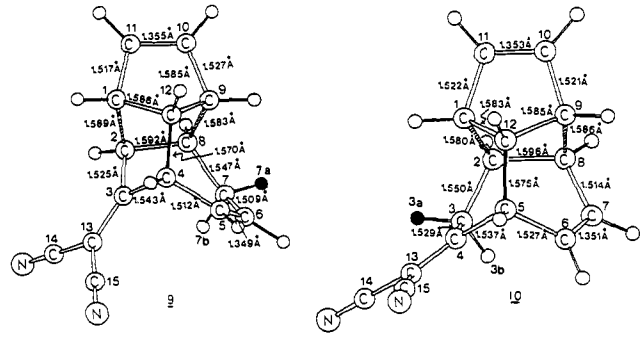

Figure 5. MNDO optimized geometries of the two cage molecules.

Michael-type addition of **6** to **1** arises from the one-site FMO interaction between LUMO+1 and the symmetric homo. In the one-site adduct **11**, the negative charge is shifted from **6** to the dicyanoheptafulvene moiety, and indeed the HOMO of **11** has the larger extension in the moiety (Figure 2), according to the resonance structures **11a**–**f** in Scheme VI. This FMO extension is insensitive to the almost free rotation of the cyclopentadienyl group around the newly formed C–C bond.[24] Thus, the HOMO shape in Figure 2 predicts the favorable protonation sites shown by the upward arrows.

(23) Another ion adduct **11′** formed by the C-7 attack at the LUMO of **1** similar to the C-1 attack of Scheme III is also examined. However, **11′** is calculated to be 23.8 kcal/mol less stable than **11** and hence unlikely.

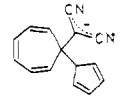

11′

(24) The MNDO energy of the rotation is calculated to be less than 2 kcal/mol.

Scheme VII

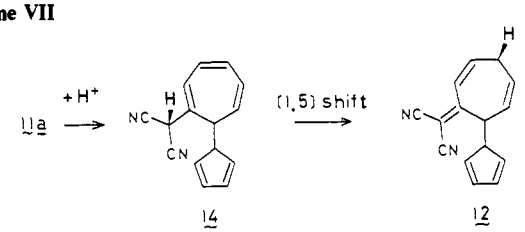

Scheme VIII

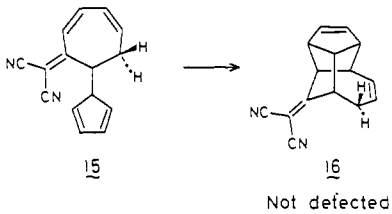

Figure 3 shows two protonated (neutral) intermediates **12** and **13**. The (**11a** + H^+) species **14** will be discussed in the last paragraph of this section. The two intermediates **12** and **13** are not sufficiently stable to be detected spectroscopically by ^1H NMR or experimentally by trapping with a strong dienophile, e.g. dimethyl acetylenedicarboxylate (DMAD). In both species **12** and **13**, the rotational energy barriers around the C–C bond connecting the five- and seven-membered rings are so small (less than 2 kcal/mol) that the subsequent intramolecular Diels–Alder (DA) reaction occurs readily. After protonation (**11** + H^+), the cycloaddition can be classified as a normal electron demand[25] DA reaction; that is, the proton and the two cyano groups activate the dienophile part of the seven-membered ring.

Figure 4 shows the two transition-state (TS) geometries of the intramolecular DA reaction. The reaction coordinate proceeds along the typical [4 + 2]-addition movement,[26] resulting in the formation of the two cage molecules **9** and **10** in Figure 5. It is noteworthy that in both molecules the C(2)–C(8) bonds are long (ca. 1.6 Å), indicating the large ring strain imposed on the bonds. This anomalously large strain is experimentally confirmed by the $^1J_{C(2)H}$ (152.8 Hz for **9**; 146.7 Hz for **10**) and $^1J_{C(8)H}$ (142.8 Hz for **9**; 149.8 Hz for **10**) coupling constants. Surprisingly, the former value in **9** is very close to that (155 Hz) of tetraprismane (cubane).[27] The large ring strain is also confirmed by the $^1J_{C(1)H}$, $^1J_{C(9)H}$, and $^1J_{C(12)H}$ coupling constants of the undeuteriated products **9** (154.4–147.5 Hz) and **10** (153.4–148.6 Hz) as well as those ($^1J_{CD}$ 23.2–21.5 Hz)[28] of the deuteriated ones (**9**-d_5 and **10**-d_5) listed in Table I. These $^1J_{CH}$ values[30] can be compared with those of pentaprismane (148 Hz),[27] dodecahedrane (134.9 Hz),[33] cyclopropane (160.3 Hz),[34] and cyclobutane (133.6 Hz).[34]

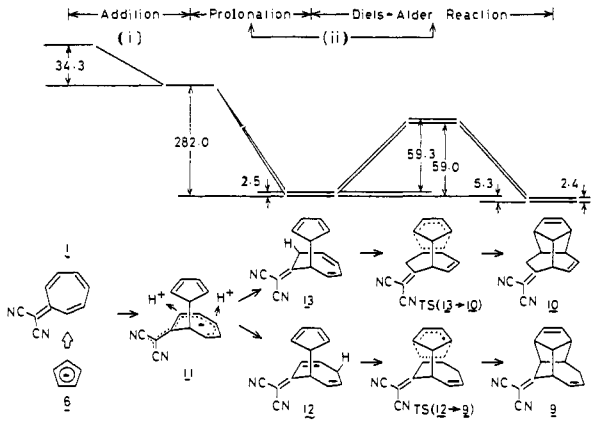

Figure 6. MNDO potential-energy diagram. Steps i and ii are defined in Scheme IV. The energy heights are in kcal/mol. The overestimated activation energies (59.3 and 59.0 kcal/mol) are reduced to 25.7 and 28.8 kcal/mol, respectively, with 3-21G//MNDO (see ref 26).

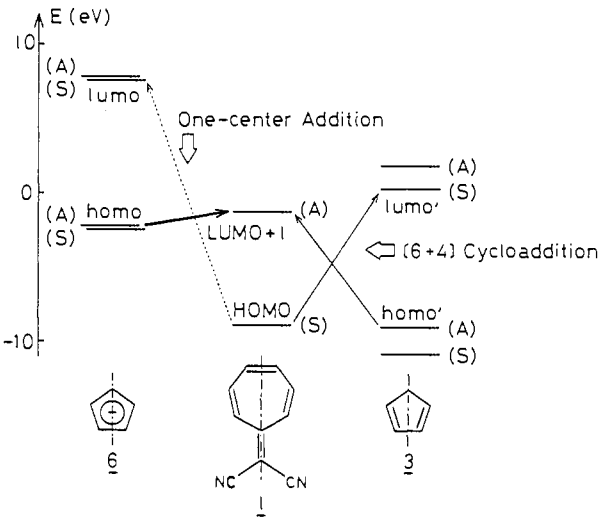

Figure 7. MNDO FMO energies of **1**, **3**, and **6**. Arrows indicate charge-transfer interactions. Abbreviations A and S denote antisymmetric and symmetric MOs, respectively, with respect to the mirror plane. For the combination (**1** + **3**), the HOMO–lumo′ energy gap is similar to the homo′-(LUMO+1) one, which leads to a concerted addition. On the other hand, for the reaction of (**1** + **6**), the HOMO–lumo gap is much larger than the homo–(LUMO+1) gap, which prohibits the concerted [6 + 4] addition and gives rise to the one-center addition.

According to the HOMO shape (i.e., the largest weight of **11a**) in Figure 2, the protonation at the carbon adjacent to the two cyano groups should be most favorable. Probably, this protonated species **14** is initially generated when the solution is neutralized by HCl. However, **14** may be converted readily to **12** through a [1,5] sigmatropic rearrangement. The HOMO shape also predicts that the concentration of **13** is larger than that of **12**, which should lead to the product distribution [**10**] > [**9**]. The dilemma between the prediction [**10**] > [**9**] and the experimental result [**10**] < [**9**] can be solved by taking into account the *precursor* **14** for **12**.

The fourth-rank intermediate **15** coming from the resonance structure **11d** would be negligible because of the HOMO shape.

(25) Sustmann, R.; Schubert, R. *Angew. Chem., Int. Ed. Engl.* **1972**, *11*, 840.

(26) The MNDO TS of DA reactions has two characteristics. One is the appearance of two imaginary frequencies corresponding to the synchronous addition in Figure 4 and the asymmetric stretching of two newly formed C–C bonds [184.2*i* cm^{-1} for TS(**12**→**9**) or 181.2*i* cm^{-1} for TS(**13**→**10**)]. For the ethylene–butadiene [4 + 2]-addition TS, the two imaginary frequencies are 1029.6*i* and 165.8*i* cm^{-1}. The other is the overestimated activation energy E_a. MNDO E_a(**12**→**9**) is 59.0 kcal/mol and E_a(**13**→**10**) is 59.3 kcal/mol, as shown in Figure 6. With the 3-21G single-point calculation on the MNDO geometry (3-21G//MNDO), they are 28.8 and 25.7 kcal/mol, respectively. For the ethylene–butadiene TS, the MNDO E_a is 49.3 kcal/mol and the 3-21G E_a is 35.9 kcal/mol. Despite the large E_a difference between MNDO and 3-21G, the geometries of the ethylene–butadiene TS are found to be quite similar. Hence, the geometries in Figure 4 are acceptable.

(27) Eaton, P. E.; Or, Y. S.; Branca, S. J. *J. Am. Chem. Soc.* **1981**, *103*, 2134–2136.

(28) The corresponding ^{13}C–^1H coupling constants are calculated by using the following equation, $J_{CH} = 6.515J_{CD}$,[29] as $^1J_{C(10)H}$ = 170.7, $^1J_{C(11)H}$ = 169.4, $^1J_{C(12)H}$ = 149.8, $^1J_{C(1)H}$ = 147.9, and $^1J_{C(9)H}$ = 140.1 Hz for **9** and $^1J_{C(10)H}$ = 168.7, $^1J_{C(11)H}$ = 169.4, $^1J_{C(12)H}$ = 145.3, $^1J_{C(1)H}$ = 151.1, and $^1J_{C(9)H}$ = 141.4 Hz for **10**, respectively (cf. observed values in Table I).

(29) Kalinowski, H.-O.; Berger, S.; Braun, S. *Carbon-13 NMR Spectroscopy*; Wiley: Chichester, England, 1988; p 488.

(30) Also, the olefinic carbon couplings—$^1J_{C(10)H}$ and $^1J_{C(11)H}$ (171.7–169.3 Hz) in both **9** and **10** and $^1J_{C(6)H}$ (170.0 Hz) in **10**—are found to be larger than those of cyclobutene (168.6 Hz)[31] and norbornene (165 Hz).[32] The other olefinic carbon couplings—$^1J_{C(5)H}$ (167.0 Hz) and $^1J_{C(6)H}$ (160.4 Hz) in **9** and $^1J_{C(7)H}$ (165.7 Hz) in **10**—are comparable to those of cyclopentene (161.6 Hz) and cyclohexene (158.4 Hz).[31]

(31) Ref 29, p 501.

(32) Marchand, A. P. *Stereochemical Applications of NMR Studies in Rigid Bicyclic Systems*; Verlag Chemie International: Deerfield Beach, FL, 1982; p 61.

(33) Ternansky, R. J.; Balogh, D. W.; Paquette, L. A. *J. Am. Chem. Soc.* **1982**, *104*, 4503–4504. Paquette, L. A.; Ternansky, R. J.; Balogh, D. W.; Kentgen, G. *J. Am. Chem. Soc.* **1983**, *105*, 5446–5450.

(34) Ref 29, p 496. Breitmeier, E.; Voelter, W. *^{13}C NMR Spectroscopy*; Verlag Chemie: Weinheim, Germany, 1974; p 139. Stothers, J. B. *Carbon-13 NMR Spectroscopy*; Academic: New York, 1972; p 343.

Table I. Selected ^{13}C NMR (100.6 MHz, $CDCl_3$, Me_4Si) Spectral Data for the Products Obtained[a,b]

	gem-dicyanoethylene				cyclopentadiene					heptafulvene					
moiety	C(3)	C(14)≡N	C(15)≡N	C(13)	C(10)	C(11)	C(12)	C(1)	C(9)	C(6)	C(5)	C(2)	C(4)	C(8)	C(7)
9	193.78 (s) [dtdd]	112.01 (s) [d]	111.31 (s) [d]	78.10 (s) [dd]	139.66 (d) [ddddd]	129.12 (d) [ddd]	62.54 (d) [dddttd]	56.93 (d) [ddddt]	46.89 (d) [ddddtd]	130.84 (d) [dtddd]	128.28 (d) [dtdd]	50.91 (d) [dddddddd]	42.18 (d) [ddtt]	38.95 (d) [dddddd]	28.98 (t) [dddddd]
	$^2J_{CH(2)}$ 2.2 $^2J_{CH(4)}$ 6.5 $^3J_{CH(12)}$ 7.2	$^4J_{CH(4)}$ 1.9	$^4J_{CH(4)}$ 1.3	$^3J_{CH(2)}$ 3.3 $^3J_{CH(4)}$ 4.1	$^1J_{CH(10)}$ 170.2 $^3J_{CH(1)}$ 7.1 $^3J_{CH(8)}$ 4.7	$^1J_{CH(11)}$ 171.7 $^3J_{CH(2)}$ <1.0 $^3J_{CH(9)}$ 6.5	$^1J_{CH(12)}$ 147.5 $^3J_{CH(2)}$ 4.7 $^3J_{CH(8)}$ 2.5	$^1J_{CH(1)}$ 148.9 $^3J_{CH(9)}$ 7.7	$^1J_{CH(9)}$ 154.4 $^3J_{CH(7a)}$ 3.2 $^3J_{CH(7b)}$ 6.8	$^1J_{CH(6)}$ 160.4	$^1J_{CH(5)}$ 167.0	$^1J_{CH(2)}$ 152.8 $^3J_{CH(4)}$ 1.6 $^3J_{CH(11)}$ <1.0 $^3J_{CH(12)}$ 5.1	$^1J_{CH(4)}$ 138.0 $^3J_{CH(2)}$ 5.3	$^1J_{CH(8)}$ 142.8 $^3J_{CH(10)}$ <1.0 $^3J_{CH(12)}$ 2.2	$^1J_{CH(7)}$ 128.0 126.2 $^3J_{CH(9)}$ 3.1 $^4J_{CH(10)}$ <1.0
9-d_5	193.76 (s) [tddd]	112.03 (s) [d]	111.32 (s) [d]	78.26 (s) [dd]	139.22[c] [tdd]	128.70[c] [t]	62.13[c] [tddtd]	56.50[c] [tt]	46.44[c] [tdtd]	130.87 (d) [dtddd]	128.33 (d) [dtdd]	50.89 (d) [ddddd]	42.13 (d) [ddtd]	38.95 (d) [ddddd]	29.03 (t) [ddddd]
					$^1J_{CD(10)}$ 26.2	$^1J_{CD(11)}$ 26.0	$^1J_{CD(12)}$ 23.0	$^1J_{CD(1)}$ 22.7	$^1J_{CD(9)}$ 21.5	$^1J_{CH(6)}$ 160.4	$^1J_{CH(5)}$ 167.0	$^1J_{CH(2)}$ 152.6	$^1J_{CH(4)}$ 138.0	$^1J_{CH(8)}$ 142.6	$^1J_{CH(7)}$ 128.0
	gem-dicyanoethylene				cyclopentadiene					heptafulvene					
moiety	C(4)	C(15)≡N	C(14)≡N	C(13)	C(10)	C(11)	C(12)	C(1)	C(9)	C(7)	C(6)	C(5)	C(8)	C(2)	C(3)
10	184.75 (s) [ddddd]	111.68 (s) [t]	111.66 (s) [t]	82.55 (s) [dt]	135.60 (d) [ddddd]	133.63 (d) [ddt]	55.06 (d) [ddtdd]	53.43 (d) [dddddd]	48.84 (d) [ddddtd]	139.45 (d) [dddtd]	127.40 (d) [ddddd]	46.58 (d) [ddddd]	40.17 (d) [dddtdt]	35.19 (d) [dttdd]	35.33 (t) [tdddd]
	$^2J_{CH(3b)}$ 4.7 $^2J_{CH(5)}$ 5.7 $^3J_{CH(2)}$ 6.6	$^4J_{CH(3a)}$ 2.0 $^4J_{CH(3b)}$ 2.0	$^4J_{CH(3a)}$ 1.7 $^4J_{CH(3b)}$ 1.7	$^3J_{CH(3a)}$ 4.7 $^3J_{CH(3b)}$ 4.7 $^3J_{CH(5)}$ 5.6	$^1J_{CH(10)}$ 169.3 $^3J_{CH(8)}$ 2.0 $^4J_{CH(2)}$ 2.3	$^1J_{CH(11)}$ 169.5 $^3J_{CH(9)}$ 6.9 $^4J_{CH(8)}$ 2.9	$^1J_{CH(12)}$ 148.6 $^3J_{CH(2)}$ 3.5 $^3J_{CH(8)}$ 5.7	$^1J_{CH(1)}$ 153.4 $^3J_{CH(3b)}$ 1.4 $^3J_{CH(9)}$ 7.2	$^1J_{CH(9)}$ 148.6 $^3J_{CH(7)}$ 2.7	$^1J_{CH(7)}$ 165.7 $^3J_{CH(9)}$ 2.0	$^1J_{CH(6)}$ 170.0	$^1J_{CH(5)}$ 142.1 $^3J_{CH(3a)}$ 3.3	$^1J_{CH(8)}$ 149.8 $^3J_{CH(12)}$ 3.0	$^1J_{CH(2)}$ 146.7 $^3J_{CH(9)}$ 3.2 $^3J_{CH(12)}$ 3.2	$^1J_{CH(3)}$ 132.3 $^3J_{CH(1)}$ 1.2 $^3J_{CH(5)}$ 4.9
10-d_5	184.81 (s) [ddddd]	111.69 (s) [t]	111.67 (s) [t]	82.46 (s) [dt]	135.10[c] [tdd] $J_{CD(10)}$ 25.9	133.13[c] [tdt] $J_{CD(11)}$ 26.0	54.55[c] [tddd] $J_{CD(12)}$ 22.3	52.91[c] [tddd] $J_{CD(1)}$ 23.2	48.27[c] [tddtd] $J_{CD(9)}$ 21.7	139.46 (d) [dddt] $J_{CH(7)}$ 165.8	127.35 (d) [dddd] $J_{CH(6)}$ 170.0	46.47 (d) [ddddd] $J_{CH(5)}$ 142.1	40.10 (d) [dddtt] $J_{CH(8)}$ 149.8	35.10 (d) [dtdd] $J_{CH(2)}$ 146.7	35.29 (t) [tddd] $J_{CH(3)}$ 132.3

[a] For the atomic numbering in **9** and **10**, see Scheme IV. Chemical shifts and coupling constants are in δ and Hz, respectively. Multiplicities in parentheses and brackets are derived from off-resonance spectra and those resolution-enhanced with Gaussian wind function, respectively. [b] Signal and coupling assignments are confirmed by SEL, gated decoupling, 2D $^{13}C-^1H$ COSY and COLOC, and LSPD spectra. The magnitudes of J_{CH} and J_{CD} are determined by gated decoupling spectra resolution-enhanced with Gaussian wind function as well as LSPD experiments with a partial aid of Karplus' dihedral angle relationship for $^3J_{CH}$. Coupling constants that are not shown in Table I are as follows. For **9**: $^2J_{C(1)H(11)}$ 8.0; $^3J_{C(1)H(8)}$ < 1.0; $^3J_{C(1)H(10)}$ 8.8; $^4J_{C(1)H(5)}$ 1.3; $^4J_{C(1)H(7b)}$ 1.3; $^2J_{C(2)H(8)}$ 2.7; $^3J_{C(2)H(7a)}$ 7.9; $^3J_{C(2)H(7b)}$ 2.3; $^3J_{C(2)H(9)}$ 3.1; $^4J_{C(2)H(10)}$ < 1.0; $^3J_{C(3)H(5)}$ 5.1; $^3J_{C(3)H(8)}$ 6.5; $^4J_{C(3)H(6)}$ < 1.0; $^2J_{C(4)H(5)}$ 5.3; $^2J_{C(4)H(12)}$ 1.3; $^3J_{C(4)H(6)}$ 10.6; $^4J_{C(4)H(7a)}$ < 1.0; $^4J_{C(4)H(7b)}$ 1.3; $^4J_{C(4)H(10)}$ < 1.0; $^4J_{C(4)H(11)}$ < 1.0; $^2J_{C(5)H(4)}$ 6.8; $^3J_{C(5)H(7a)}$ 6.8; $^3J_{C(5)H(7b)}$ 5.1; $^4J_{C(5)H(1)}$ < 1.0; $^4J_{C(5)H(8)}$ 1.4; $^2J_{C(6)H(5)}$ 1.4; $^2J_{C(6)H(7a)}$ 8.2; $^2J_{C(6)H(7b)}$ 8.2; $^3J_{C(6)H(4)}$ 6.4; $^3J_{C(6)H(8)}$ 5.9; $^2J_{C(7)H(6)}$ 4.6; $^2J_{C(7)H(8)}$ 2.1; $^3J_{C(7)H(5)}$ 9.9; $^2J_{C(8)H(7a)}$ 3.3; $^2J_{C(8)H(7b)}$ 5.3; $^3J_{C(8)H(6)}$ 6.6; $^4J_{C(8)H(4)}$ 1.4; $^4J_{C(8)H(11)}$ < 1.0; $^2J_{C(9)H(10)}$ 6.3; $^3J_{C(9)H(2)}$ 3.2; $^3J_{C(9)H(4)}$ 1.9; $^3J_{C(9)H(11)}$ 8.2; $^2J_{C(10)H(9)}$ 1.6; $^2J_{C(10)H(11)}$ 2.4; $^4J_{C(10)H(2)}$ < 1.0; $^4J_{C(10)H(4)}$ < 1.0; $^2J_{C(11)H(10)}$ 3.3; $^2J_{C(12)H(4)}$ 1.6; $^3J_{C(12)H(10)}$ 4.5; $^3J_{C(12)H(11)}$ 3.1; $^4J_{C(12)H(7a)}$ 3.1; $^4J_{C(12)H(7b)}$ 2.5; $^4J_{C(13)H(8)}$ < 1.0. For **10**: $^3J_{C(1)H(5)}$ 3.0; $^3J_{C(1)H(8)}$ 2.3; $^3J_{C(1)H(10)}$ 9.4; $^2J_{C(2)H(3a)}$ 4.2; $^2J_{C(2)H(3b)}$ 2.9; $^3J_{C(2)H(7)}$ 4.2; $^4J_{C(2)H(5)}$ 1.5; $^2J_{C(3)H(2)}$ 1.4; $^3J_{C(3)H(8)}$ 1.9; $^2J_{C(4)H(3a)}$ 5.4; $^4J_{C(4)H(7)}$ 1.8; $^2J_{C(5)H(6)}$ 6.1; $^3J_{C(5)H(3b)}$ 1.6; $^3J_{C(5)H(7)}$ 9.1; $^4J_{C(5)H(10)}$ < 1.0; $^4J_{C(5)H(11)}$ < 1.0; $^2J_{C(6)H(5)}$ 5.8; $^2J_{C(6)H(7)}$ 2.4; $^3J_{C(6)H(8)}$ 6.3; $^3J_{C(6)H(12)}$ 1.4; $^2J_{C(7)H(6)}$ 2.4; $^2J_{C(7)H(8)}$ 4.5; $^3J_{C(7)H(2)}$ 2.4; $^3J_{C(7)H(5)}$ 6.7; $^2J_{C(8)H(2)}$ 1.5; $^2J_{C(8)H(7)}$ 3.2; $^3J_{C(8)H(3a)}$ 5.7; $^3J_{C(8)H(3b)}$ 3.2; $^3J_{C(8)H(6)}$ 10.3; $^4J_{C(8)H(5)}$ 1.5; $^2J_{C(9)H(10)}$ 5.7; $^3J_{C(9)H(2)}$ 1.6; $^3J_{C(9)H(5)}$ 3.3; $^3J_{C(9)H(11)}$ 8.3; $^4J_{C(9)H(3a)}$ 1.8; $^4J_{C(9)H(3b)}$ 1.8; $^2J_{C(10)H(9)}$ 1.2; $^3J_{C(10)H(1)}$ 7.9; $^2J_{C(11)H(10)}$ 2.9; $^4J_{C(11)}H_{(3a)}$ < 1.0; $^4J_{C(11)H(5)}$ < 1.0; $^3J_{C(12)H(10)}$ 3.5; $^3J_{C(12)H(11)}$ 2.7; $^4J_{C(12)H(3b)}$ 1.5; $^4J_{C(13)H(2)}$ < 1.0; $^4J_{C(13)H(12)}$ < 1.0. [c] Small abundant triplet.

Table II. Selected ^{1}H NMR (400 MHz, $CDCl_3$, Me_4Si) Spectral Data for the Products Obtained[a,b]

compd	H(10)	H(5)	H(11)	H(6)	H(4)	H(1)	H(2)	H(12)	H(7a)	H(9)	H(7b)	H(8)
9	6.40 (dd) [dddd]	6.08 (td) [dddd]	5.91 (dd) [ddt]	5.69 (ddd) [ddddd]	3.33 (dd) [dddd]	3.08 (br s) [dddd]	3.04 (dt) [ddd]	2.59 (br d) [ddddd]	2.55 (dt) [dddd]	2.49 (br s) [dddd]	2.24 (ddt) [dddd]	2.02 (br t) [ddddq]
9-d_5		6.08 (td) [dddd]		5.69 (ddd) [ddddd]	3.34 (d) [ddd]		3.04 (dd) [dd]		2.56 (dt) [dddd]		2.24 (ddt) [dddd]	2.02 (br t) [dddd]
					$J_{4,12}$ 5.2	$J_{1,9}$ 1.7	$J_{2,4}$ 1.5	$J_{2,12}$ 1.3	$J_{7a,8}$ 6.0	$J_{8,9}$ < 1.0	$J_{7b,8}$ 1.3	$J_{8,12}$ 1.0
compd	H(7)	H(10)	H(11)	H(6)	H(5)	H(3a)	H(3b)	H(12)	H(1)	H(8)	H(9)	H(2)
10	6.46 (t) [ddd]	6.15 (ddd) [ddd]	6.11 (dd) [dddd]	5.75 (ddd) [ddd]	3.83 (dd) [dddd]	2.87 (dd) [ddt]	2.81 (dd) [dd]	2.42 (dddd) [ddddd]	2.38 (br s) [ddddd]	2.32 (br t) [ddddd]	2.14 (br dd) [ddddd]	1.93 (ddt) [ddtd]
10-d_5	6.45 (t) [dddd]			5.75 (ddd) [ddd]	3.83 (d) [dddd]	2.87 (dd) [ddd]	2.81 (dd) [ddd]			2.31 (br t) [ddd]		1.93 (ddd) [dddd]
					$J_{3a,5}$ 0.8	$J_{2,3a}$ 4.5	$J_{2,3b}$ 2.5	$J_{9,12}$ 2.6	$J_{1,12}$ 4.5	$J_{8,12}$ 1.7	$J_{1,9}$ 0.7	$J_{2,12}$ 2.5

[a] The numbering for hydrogens follows that for carbons in Scheme IV. Chemical shifts and selected coupling constants are in δ and Hz, respectively. Multiplicities in parentheses and brackets are due to Lorentz-transformed ^{1}H NMR and those resolution-enhanced with sine-bell wind function, respectively. [b] Coupling constants that are not shown in Table II are as follows. For **9**: $J_{1,10}$ 0.7; $J_{1,11}$ 2.9; $J_{1,12}$ 2.3; $J_{2,8}$ 6.2; $J_{4,5}$ 8.4; $J_{4,6}$ 0.5; $J_{4,10}$ < 1.0; $J_{4,11}$ < 1.0; $J_{5,6}$ 9.8; $J_{5,7a}$ 0.8; $J_{5,7b}$ 3.1; $J_{6,7a}$ 6.9; $J_{6,7b}$ 1.9; $J_{6,8}$ 0.8; $J_{7a,7b}$ 18.7; $J_{8,10}$ 0.8; $J_{8,11}$ 0.8; $J_{9,10}$ 3.4; $J_{9,11}$ 0.8; $J_{9,12}$ 1.6; $J_{10,11}$ 5.6; $J_{11,12}$ < 1.0. For **10**: $J_{1,3a}$ 0.8; $J_{1,10}$ 1.3; $J_{1,11}$ 2.6; $J_{2,7}$ < 1.0; $J_{2,8}$ 7.5; $J_{2,9}$ 0.5; $J_{3a,3b}$ 18.7; $J_{3b,5}$ < 1.0; $J_{5,6}$ 6.2; $J_{5,7}$ 1.5; $J_{5,12}$ 8.2; $J_{6,7}$ 7.7; $J_{6,8}$ 1.4; $J_{7,8}$ 7.1; $J_{7,9}$ < 1.0; $J_{8,11}$ 0.8; $J_{9,10}$ 3.4; $J_{9,11}$ 1.1; $J_{10,11}$ 5.8; $J_{10,12}$ < 1.0. The assignment of all the couplings is based on 2D NMR ^{1}H-^{1}H COSY and COLOC spectra as well as ^{1}H-^{1}H homonuclear decoupling experiments. Magnitudes of $J_{H,H}$ are determined from ^{1}H NMR spectra treated with Gaussian and sine-bell wind functions. Coupling constants represented as <1.0 Hz are confirmed by 2D NMR ^{1}H-^{1}H COLOC spectra and decoupling experiments.

In fact, the subsequent DA adduct **16** (Scheme VIII) has not been detected.

Concluding Remarks

The present *one-pot* reaction of 8,8-dicyanoheptafulvene (**1**) with cyclopentadienide anion (**6**) leading to strained cage molecules is in remarkable contrast to the reported reaction of tropone and **6** in Scheme III. Figure 6 shows the mechanism derived from the MNDO calculations. In the first step, an ionic adduct **11** is formed via the attack of the cyclopentadienide anion (**6**) at the C-1 position of 8,8-dicyanoheptafulvene (**1**) according to the LUMO+1 shape. When the solution of **11** is neutralized with acid, two intermediates **12** and **13** are formed as the second step from **11c** and **11b**, respectively. The formation of these two intermediates is predicted by the HOMO shape of **11**. The third step is a normal electron demand intramolecular DA addition, which gives cage molecules **9** and **10**. The MNDO energy, although somewhat qualitative, has shown that two routes are equally likely (Figure 6). Experimentally, **9** is the main product and **10** is the minor (ca. 4:1). Protonation at the two favorable sites of **11** in Figure 2 leads to the two cage molecules.

The present mechanism is entirely different from those in Schemes II and III. Why does the reaction of **1** and **6** as well as that of **2** and **6** not give the [6 + 4] cycloadduct? As shown in Figure 1, a symmetry-allowed (in-phase) FMO overlap may be obtained in the [6 + 4] configuration. This apparent curiosity is ascribed to the FMO energy levels shown in Figure 7. For the concerted cycloaddition, the magnitude of the charge transfer (CT) and back-CT should be comparable. That is, the energy gap for CT should be similar to that for back-CT. While the combination of **1** and **3** satisfies this condition, that of **1** and **6** does not. The reaction therefore proceeds through a one-site addition via the almost exclusively one-directional homo → (LUMO+1) CT. The second question is concerned with comparison of the reactivity of substrates **1** and **2** toward **6**. The one-site adduct anion would be commonly generated. The crucial difference lies in its subsequent protonation. While the present intermediate **11** reacts under FMO control, the anion intermediate from reaction of **2** and **6** is charge controlled. The proton is attached to the oxygen atom (Scheme III), and the normal electron demand condition for the intramolecular DA addition is therefore not given. In this respect, the exocyclic dicyanomethylene group is indispensable for the intramolecular DA reaction.

Experimental Section

General. 8,8-Dicyanoheptafulvene (**1**) was prepared according to a literature method.[5b] Hexadeuteriocyclopentadiene (cyclopentadiene-d_6) was prepared by a modified method of a literature procedure.[35] The deuteriation was repeated five times, and the resulting cyclopentadiene-d_6 was used immediately after distillation [bp 38 °C; isotopic purity > 98% from ^{1}H NMR (90 MHz) spectroscopy[36]]. Hexamethylphosphoric triamide used for the deuteration was treated with barium oxide overnight and then distilled in vacuo (bp 74–75 °C/3 mmHg). All other solvents were freshly distilled under nitrogen from appropriate drying agents. Deuterium oxide (isotopic purity: 99.97%) (Merck) and sodium deuteroxide in D_2O (Merck) were used for deuterium-labeling of cyclopentadiene. For preparative thin-layer chromatography, silica gel (0.063–0.200 mm) (Merck Kieselgel 60) was employed.

Melting points were determined on a Büchi 511 apparatus in open capillary tubes and are uncorrected. Elemental analyses were performed at the Analytical Laboratory, Department of Chemistry, the University of Tokyo, Hongo, Tokyo. IR spectra were recorded on a Hitachi 260-50 spectrometer. UV and visible spectra were taken with a Hitachi EPS-3T recording spectrometer using 1-cm quartz cells. Mass spectra were obtained with a JEOL DM-303 double focusing spectrometer and are reported as m/z values for significant ions with relative intensities in parentheses (% for the base peak) for low-resolution analyses.

^{13}C and ^{1}H NMR spectra were measured in degassed and sealed 5-mm tubes (ca. 0.2 and 0.06 M solutions of the products in $CDCl_3$, respectively) on a Bruker AM400 instrument at the Chemical Analysis Center, Saitama University. Chemical shifts (δ) are reported downfield from the internal standard Me_4Si. The observed 100.6-MHz ^{13}C and 400-MHz ^{1}H NMR data are listed in Tables I and II, respectively. One-dimensional ^{1}H NMR spectra were recorded without and with the resolution enhancement by Gaussian and sine-bell wind functions, separately, at 64K data points. The ^{13}C NMR with CPD[2] and with proton off-resonance spectra were taken with 32K data points. Gated decoupling and LSPD[21] spectra were obtained without and with the resolution enhancement by the Gaussian wind function (128K data points, acquisition time 2.621 s). The LSPD and ^{13}C-^{1}H SEL spectra were recorded with a decoupler power of 0.25 and 14.68 mG, respectively. The LSPD spectra were obtained with a flip angle of 45°, repetition time of 2.644 s, and 10000–20000 accumulations.

2D NMR ^{1}H-^{1}H COSY, ^{13}C-^{1}H COSY, ^{1}H-^{1}H COLOC, and ^{13}C-^{1}H COLOC spectra were measured using conditions similar to those in the literature.[16-19] The experimental details for each type of spectroscopy are described in the supplementary material. The 2D contour maps are composed of $256(f_1) \times 1024(f_2)$ and $128(f_1) \times 4096(f_2)$ data-point spectra for ^{1}H-^{1}H and ^{13}C-^{1}H correlations, respectively. The ^{13}C-^{1}H COLOC contour diagrams were recorded with $128(f_1) \times 4096(f_2)$ data points with three different polarization delays of 50, 100, and 150 ms, separately, to obtain accurate analytical results.

Reaction of 8,8-Dicyanoheptafulvene (1) with Cyclopentadienide Anion (6). A solution of 8,8-dicyanoheptafulvene (1.927 g, 12.5 mmol) in 10 mL of anhydrous THF at -30 °C was added dropwise over a period of 10 min to a freshly prepared solution of cyclopentadienide anion [70 mmol, from 5 mL of cyclopentadiene and 1.68 g (70 mmol) of sodium hydride] in 100 mL of anhydrous THF. After the reaction mixture was stirred for 4 h at -30 °C, 12 mL of 6 N hydrochloric acid was added dropwise slowly to the reaction mixture at -10 °C and then the reaction mixture was stirred for 30 min. The mixture was then poured onto 300 mL of ice–water and extracted several times with ether (300 mL). The combined organic phases were dried over magnesium sulfate. Solvent removal under reduced pressure gave 3.039 g of an oily material. Kugelrohr distillation (100 °C, 4.4 mmHg) gave a volatile material and left

(35) Gallinela, E.; Mirone, P. *J. Labelled Compd.* **1971**, *7*, 183–184.

(36) For routine ^{1}H NMR spectroscopy, Hitachi R-24B (60 MHz) and JEOL FX-90Q (90 MHz) instruments were used.

a viscous oil (2.86 g). The IR and ^{1}H NMR (60 MHz) spectra of the volatile material were identical with those of cyclopentadiene contaminated with a small amount of dicyclopentadiene. The viscous oil was chromatographed on silica gel (33 × 5.5 cm i.d.) and eluted with benzene followed by chloroform. Chloroform elution gave 2.265 g of the product mixture, which was separated into two components **9** (R_f 0.38, 1.707 g, 62%) and **10** (R_f 0.45, 463 mg, 17%) by preparative thin-layer chromatography developed with hexane–ethyl acetate (9:1). Each component was collected and recrystallized from ethanol to give colorless prisms **9** and **10**.

9: mp 80–81 °C; IR (KBr) ν_{max} 3055 (w), 3040 (w), 3025 (w), 2955 (w), 2930 (m), 2230 (vs), 1640 (m), 1615 (vs), 1435 (m), 1380 (m), 1335 (m), 1260 (m), 924 (m), 835 (m), 770 (m), 730 (vs), 619 (m), 588 (m) cm^{-1}; UV-vis λ_{max} (EtOH) 230 (log ϵ 3.91), 272 nm (3.92); EI-MS (75 eV) *m/z* (relative intensity) 221 (M^+ + 1, 11), 220 (M^+, 62), 219 (22), 192 (22), 179 (17), 165 (14), 155 (95), 154 (100), 142 (54), 128 (52), 127 (19), 115 (18), 101 (11), 91 (16), 79 (26), 78 (16), 77 (26), 66 (15), 65 (17), 51 (12), 39 (23). Anal. Calcd for $C_{15}H_{12}N_2$: C, 81.79; H, 5.49; N, 12.72. Found: C, 81.84; H, 5.28; N, 12.64.

10: mp 96–97 °C; IR (KBr) ν_{max} 3060 (w), 3050 (w), 2970 (s), 2950 (m), 2235 (vs), 1585 (vs), 1407 (m), 1328 (m), 778 (s), 740 (m), 709 (s), 695 (s) cm^{-1}; UV-vis λ_{max} (EtOH) 237 (log ϵ 4.05), 285 nm (3.73); EI-MS (75 eV) *m/z* (relative intensity) 221 (M^+ + 1, 10), 220 (M^+, 48), 219 (17), 192 (13), 179 (11), 165 (4), 155 (100), 154 (88), 142 (17), 128 (50), 127 (12), 115 (16), 101 (16), 91 (18), 79 (17), 78 (16), 77 (27), 66 (16), 65 (17), 51 (13), 39 (18). Anal. Calcd for $C_{15}H_{12}N_2$: C, 81.79; H, 5.49; N, 12.72. Found: C, 81.86; H, 5.34; N, 12.76.

Reaction of 8,8-Dicyanoheptafulvene (1) with Sodium Cyclopentadienide-d_5. In a similar way, a solution of 2.02 g (13.1 mmol) of 8,8-dicyanoheptafulvene in 100 mL of anhydrous THF was reacted with sodium cyclopentadienide-d_5 [generated from 2.0 mL (22.3 mmol) of cyclopentadiene-d_6 and 600 mg of sodium hydride in 20 mL of anhydrous THF] at -30 °C for 3 h. Workup and purification as described above gave 1.903 g (64.5%) of the main product **9**-d_5 and 0.744 g (25%) of the minor one **10**-d_5.

9-d_5: mp 76–77 °C; IR (KBr) ν_{max} 3040 (w), 2980 (w), 2935 (w), 2830 (w), 2230 (vs), 1640 (m), 1615 (vs), 1430 (m), 1380 (m), 1280 (m), 810 (m), 770 (m), 720 (m), 700 (s), 610 (w), 580 (vs) cm^{-1}; UV-vis λ_{max} (EtOH) 230 (log ϵ 3.91), 272 nm (3.92); EI-MS (75 eV) *m/z* (relative intensity) 226 (M^+ + 1, 5), 225 (M^+, 30), 224 (14), 197 (3), 184 (2), 170 (2), 160 (4), 155 (61), 154 (100), 142 (31), 128 (31), 127 (5), 115 (3), 101 (5), 91 (2), 84 (14), 83 (11), 78 (3), 77 (9), 71 (9), 70 (11), 51 (4), 42 (6).

10-d_5: mp 97–98 °C; IR (KBr) ν_{max} 3045 (m), 2970 (s), 2955 (m), 2235 (vs), 1585 (vs), 1407 (s), 1334 (m), 1305 (m), 775 (m), 755 (m), 726 (vs), 715 (s), 695 (m), 685 (m) cm^{-1}; UV-vis λ_{max} (EtOH) 237 (log ϵ 4.05), 285 nm (3.73); EI-MS (75 eV) *m/z* (relative intensity) 226 (M^+ + 1, 10), 225 (M^+, 53), 224 (27), 223 (11), 197 (7), 184 (5), 170 (4), 160 (7), 155 (100), 154 (97), 142 (16), 128 (68), 127 (12), 120 (9), 103 (15), 96 (16), 79 (11), 78 (35), 77 (10), 71 (23), 70 (11), 51 (8), 44 (21).

Computational Methods. MO calculations were performed on a HITAC M-680H computer at the Institute for Molecular Science, Okazaki, Japan. MNDO calculations were also carried out with an ACOS 430-70 computer of the Computer Center, Nara University, Japan. Geometry optimizations were done with the MNDO MO method[37] implemented in the AMPAC program package.[38]

Acknowledgment. The authors thank the Institute for Molecular Science for the allotment of CPU time of the HITAC M-680H computer. Support of this work by Scientific Grants-in-Aid from the Ministry of Education, Science, and Culture, Japan is gratefully acknowledged.

Supplementary Material Available: NMR spectral charts for the reported compounds **9**, **9**-d_5, **10**, and **10**-d_5 [400-MHz ^{1}H NMR (Lorentz-transformed spectra and those resolution-enhanced with Gaussian and sine-bell wind functions, separately), 2D NMR ^{1}H–^{1}H COSY and ^{1}H–^{1}H COLOC, 100.6-MHz ^{13}C NMR with CPD, gated decoupling (Lorentz-transformed and resolution-enhanced with Gaussian wind function), 2D NMR ^{13}C–^{1}H COSY and ^{13}C–^{1}H COLOC, and ^{13}C NMR with LSPD spectra] and Z-matrices of MNDO optimized geometries of **1**, **6**, **11**, **12**, **13**, TS (**13** → **10**), TS(**12** → **9**), **9**, and **10** (120 pages). Ordering information is given on any current masthead page.

(37) Dewar, M. J. S.; Thiel, W. *J. Am. Chem. Soc.* **1977**, *99*, 4899–4907.
(38) AMPAC program, QCPE No. 523, Department of Chemistry, Indiana University, Bloomington, IN 47405.

Access to Naturally Occurring Cyclooctanoids by Two-Carbon Intercalation. Total Synthesis of (+)-Ceroplastol I†

Leo A. Paquette,* Ting-Zhong Wang, and Nha Huu Vo

Contribution from the Evans Chemical Laboratories, The Ohio State University, Columbus, Ohio 43210. *Received September 30, 1992*

Abstract: An enantioselective synthesis of the complete dicyclopenta[*a*,*d*]cyclooctane array represented by the sesterterpene (+)-ceroplastol-I is reported. Conversion of the readily accessible optically pure keto ketal **7** (>99% ee) to the α-methoxy derivative **9** was accomplished by adaptation of a protocol developed earlier by Patel and Reusch. Once the transposed enone **10** became available, its peracid oxidation and thermal activation afforded the lactone aldehyde **11**. Sequential Wittig and Tebbe olefination of this intermediate set the stage for Claisen rearrangement and the generation of **13**. Epimerization to set the trans B/C ring geometry was followed by a four-step carbonyl transposition to furnish the pivotal intermediate **17**. Application of the Piers cyclopentannulation scheme to **17** made **19** conveniently available. Kinetic deprotonation of **19**, formation of the less substituted enol triflate, and exposure to lithium dimethyl cuprate gave **20**. To introduce the remaining side chain, **20** was converted by conventional means into **21**, and this enone was subjected to 1,4-addition with the appropriately functionalized cuprate. Reductive removal of the cyclopentanone carbonyl in **22** delivered the target molecule **4**. The more significant developments made in the course of this undertaking are associated with the Claisen ring expansion, the carbonyl transposition in a 4-cyclooctenone without concurrent transannular bonding, and the stereocontrol attainable in bond constructions involving the α,β-unsaturated ketone functionality in **17**.

The discovery as early as 1965 of a class of closely related di- and sesterterpenes constituted of the structurally unusual dicyclopenta[*a*,*d*]cyclooctane ring system has provided considerable impetus for the development of new synthetic strategies in medium ring chemistry.[1] The ceroplastins represented by albolic acid (**1**),[2]

† This paper is dedicated to Professor Melvin S. Newman on the occasion of his 85th birthday.

(1) Review: Petasis, N. A.; Patane, M. A. *Tetrahedron* **1992**, *48*, 5757.

0002-7863/93/1515-1676$04.00/0